Composites Part B 216 (2021) 108842

Contents lists available at ScienceDirect

Composites Part B

journal homepage: www.elsevier.com/locate/compositesb

Using ultra-thin interlaminar carbon nanotube sheets to enhance the mechanical and electrical properties of carbon fiber reinforced polymer composites

Pratik Koirala [a], Nekoda van de Werken [b], Hongbing Lu [c], Ray H. Baughman [d], Raquel Ovalle-Robles [d], Mehran Tehrani [a,*]

[a] Walker Department of Mechanical Engineering, The University of Texas at Austin, Austin, TX, 78712, United States
[b] Department of Mechanical Engineering, The University of New Mexico, Albuquerque, NM, 87131, United States
[c] Department of Mechanical Engineering, The University of Texas at Dallas, Richardson, TX, 75080, United States
[d] Alan G. MacDiarmid NanoTech Institute, The University of Texas at Dallas, Richardson, TX, 75080, United States

ARTICLE INFO

Keywords:
Polymer-matrix composites (PMCs)
Carbon nanotube sheets
Interlaminar properties
Carbon fiber composites
Electrical conductivity

ABSTRACT

A major shortcoming of carbon fiber reinforced polymer composites (CFRP) is their interlaminar performance. This study provides an inexpensive and readily scalable solution to this problem by incorporating ultra-thin sheets of carbon nanotubes (CNT) between the plies (laminates) of CFRPs. To this end, dry carbon fiber fabrics are first sandwiched between CNT sheets. The fabrics are then stacked and infused with epoxy to form a CFRP with interlaminar CNT sheets. Contrary to the typical approach where microns-long CNTs are distributed randomly within a CFRP for reinforcement, this study uses ~100 nm thick CNT sheets consisting of aligned and ultra-long (0.3 mm) nanotubes. Despite their negligible weight fraction of only 0.016%, the interlaminar CNT sheets enhanced the CFRP's flexural strength by 49%, interlaminar shear strength by 30%, and mode I fracture toughness by 30%. X-ray micro-tomography revealed that samples with interlaminar CNTs are significantly resistant to delamination and crack propagation. Moreover, the in-plane electrical conductivity of these composites increased commensurate with the weight fraction of CNTs, providing a maximum enhancement of 278% over the reference sample for 0.048 wt% of CNT sheets. This study reveals that for almost no change in weight and thickness, interlaminar CNT sheets can enhance the electrical conductivity and interlaminar performance of CFRPs.

1. Introduction

Carbon fiber reinforced polymer composites (CFRP) are widely used in weight-critical structural applications due to their superior specific strength and stiffness. While CFRPs exhibit excellent in-plane performance, their interlaminar properties are relatively low. These properties are primarily dominated by the matrix and fiber-matrix interfacial characteristics. Therefore, a third material is usually added to the resin or between the laminates to alleviate CFRP's interlaminar performance [1–4]. These approaches usually result in enhanced resistance to delamination initiation and growth [5–10].

The most common methods for improving interlaminar performance of CFRPs are adding toughening particles to the resin before infusion [1,3,5,9,11–14], incorporating reinforcing particles in the interlaminar regions [15,16], coating fibers with a tough resin or nanoparticles [2,17,18], and interleaving laminates with thin sheets that have favorable chemical or physical properties [4,10,19,20]. While both micro- and nano-particles can be used to enhance the CFRP's interlaminar properties [21], using nanoparticles has proved to be more effective. Micro-scale particles or interleaving layers are usually less efficient and add undesired weight and thickness, leading to reduced in-plane properties [22,23]. Reinforcing the interlaminar interfaces using nanomaterials has, therefore, attracted great interest as it has a small effect on weight/thickness and doesn't impede the flow of resin during infusion [1,2,5–7,19,24–27]. Nanomaterials can be incorporated into polymer composites using three well-known techniques, as discussed over the following three paragraphs.

The first approach involves the direct mixing of nanomaterials in the

* Corresponding author.
E-mail address: tehrani@utexas.edu (M. Tehrani).

https://doi.org/10.1016/j.compositesb.2021.108842
Received 25 June 2020; Received in revised form 20 March 2021; Accepted 23 March 2021
Available online 2 April 2021

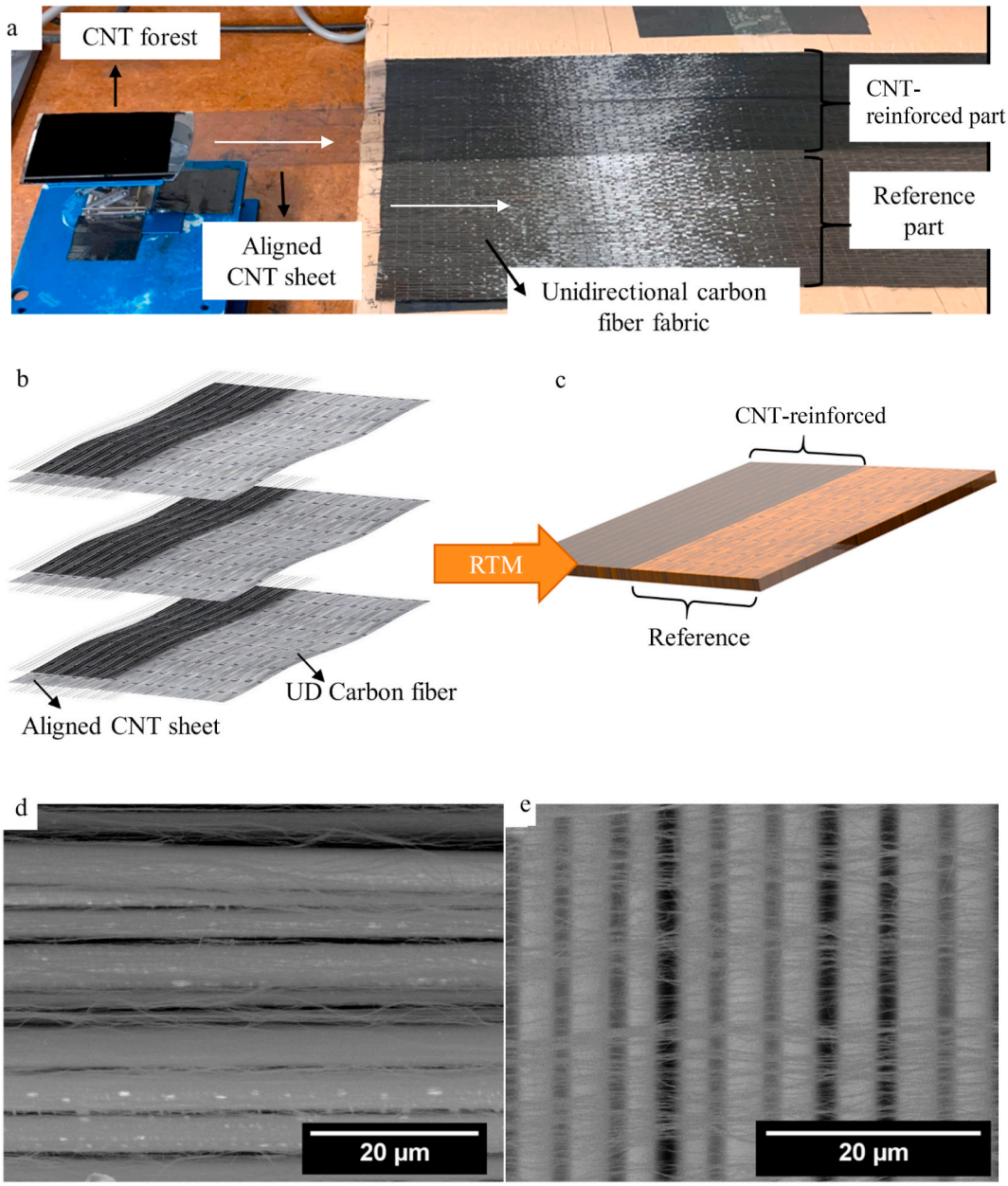

Fig. 1. a) The process of placing an aligned CNT sheet on top of a unidirectional carbon fiber fabric. The white horizontal arrows show the directions of CNT and carbon fiber alignments, respectively. b) and c) Schematics of interlaminar CNT sheets and the composite fabrication process: b) unidirectional (UD) carbon fiber fabrics are sandwiched with CNT sheets and then stacked; half of the fabrics were not CNT reinforced and used as the reference. c) fabricated composite sample showing CNT reinforced and reference portions. SEM micrographs of CNT sheets d) parallel and e) perpendicular to carbon fibers. Carbon fibers are ~7 μm in diameter, and CNTs are ~10 nm in diameter. CNT bundles seen in the figures consist of hundreds of nanotubes.

polymer matrix before infusion. Han et al. improved the interlaminar shear strength (ILSS) of a CFRP by 8% via incorporation of 0.1 wt% graphene oxide into the epoxy matrix [12]. Incorporating nanomaterials into composites requires dispersing them in the polymer matrix. Major drawbacks of this approach are the difficulty and cost associated with dispersing nanomaterials, limitations in the amount and aspect ratio of nanomaterials that can be used, and the extra processing steps required to include these nanomaterials [13].

The second approach involves fiber-matrix interface modification through the direct attachment of nanomaterials to the fiber surfaces. Zhao et al. found fiber-matrix interface modification to be more effective than matrix modification. They showed that the addition of 0.15 wt% CNTs to the fiber surfaces led to an improvement of 45% and 19% in the fiber-matrix interfacial shear strength (IFSS) and ILSS of a CFRP, respectively [28]. Mixing an identical amount of CNTs (0.15 wt%) in the matrix improved IFSS and ILSS of the same CFRP by only 10% and 15%, respectively. Cheng et al. reported that coating the carbon fibers with 1 wt% graphene nanoparticles increases the ILSS of the resulting CFRP by 37% [2]. Storck et al. adopted a chemical vapor deposition (CVD) method to grow 0.2 wt% CNTs onto carbon fibers resulting in a 37% increase of the ILSS over the reference samples [27]. Yao et al. found that the addition of 0.4 wt% vapor-grown carbon nanofibers on carbon fiber fabrics improves the ILSS of the examined CFRPs by 73% and their flexural strength by 21% [17]. It has also been shown that CNTs grown directly on carbon fiber fabrics improve the impact damage resistance and energy dissipation in CFRPs [29,30]. Direct deposition of carbon nanostructures, via some form of CVD, requires energy-intensive and high-temperature processing that often degrades the in-plane properties

at the cost of interlaminar enhancement [14]. Despite the challenges with their incorporation into composites, carbon nanomaterials offer a substantial surface area and tailorable chemical compatibility with both the polymer and fiber.

The third approach involves interlaminar modification of composites through interleaving (adding thin sheets of a different material between the laminates) with nanomaterials. Recent studies have demonstrated major improvements in mechanical performance of composites by interleaving laminates with nanofiber veils [5,6,16,26,31–33]. Interleaving with nanofiber veils improves their CFRP's delamination and crack propagation resistance, thereby enhancing their fracture toughness [1–10]. Beckerman et al. found a 173% improvement in Mode I and 69% in Mode II interlaminar fracture toughness, and 12% in ILSS of a polymer composite interleaved with nylon nanofiber veils of 4.5 gsm (g/m^2) [5]. Beylergil et al. reported that the incorporation of 1 gsm (corresponding to 0.3 wt% of the composite) nylon nanofibers at interlaminar interfaces in a CFRP increased its flexural strength by 16% and mode I fracture toughness by 50% [6]. Garcia et al. reported that incorporating 1 wt% vertically aligned CNTs at the interlaminar interfaces improved mode I and mode II interlaminar fracture toughnesses of the polymer composite system by 100% and 200%, respectively [34]. Interlaminar nano-veils can improve the impact damage resistance [35], delamination [7], and fatigue life [36,37] of composites via nanofiber bridging of micro-cracks [25,26]. In a recent study, interleaving a CFRP with 30 μm thick CNT sheets resulted in a 60% improvement in its mode I fracture toughness [38]. Interleaving laminated composites with nanomaterials sheets is simple, scalable, and highly effective in improving their interlaminar properties [1–4]. The existing interleaving methods, however, have a weight penalty of 1–10% (Supplementary Material Table S1), and their effects on the in-plane mechanical properties are generally not studied.

The present work investigates a cost-effective and scalable approach for integrating CNT sheets (~100 nm in thickness and potentially costing a few cents per m^2) between composite laminates, resulting in virtually no weight and thickness changes. The CNT sheets are dry-processed and do not require any dispersion [39]. The aligned CNT sheets are drawn from pre-grown CNT forests and introduced at interlaminar interfaces prior to composite fabrication. The effects of interlaminar CNT sheets on flexural, interfacial shear, Mode I interlaminar fracture toughness, and electrical conductivity of a CFRP are investigated in this paper. The failure mechanisms in composites interleaved with (reinforced with interlaminar) CNT sheets are elucidated.

2. Experimental

2.1. Materials

Commercial polyacrylonitrile (PAN)-derived, non-crimped unidirectional (UD) fabrics (Carbon Fiber Fabric 12k 5.7oz/193gsm UNI-Directional Hexcel IM2) were used. Aeropoxy PR2032 resin and PH3670 hardener (PTM&W Industries, Inc) were used as the matrix. Ultra-high purity (>99%) multi-walled CNT sheets were drawn from vertically aligned, 0.3 mm-tall CNT forests (acquired from Lintec NSTC) grown on a silicon substrate. The sheet has an aerial density of ~0.025 gsm, and the constituent CNTs are 10 nm in diameter [40].

2.2. Fabrication

Highly aligned CNT sheets, drawn from vertically aligned CNT forests, were placed on top and bottom of the carbon fiber fabrics, as shown in Fig. 1. Five layers of carbon fiber-CNT fabrics were stacked together ($[0^\circ]_5$) to fabricate a 1 mm thick coupon for flexural testing. Fifteen carbon fiber-CNT fabrics were stacked ($[0^\circ]_{15}$) to make a 3 mm thick coupon for short beam shear (SBS) testing. To prepare the double-cantilever beam (DCB) specimens, for Mode I interlaminar fracture toughness characterization, fourteen CNT-carbon fiber fabrics were stacked ($[0^\circ]_{14}$). A non-porous release film was inserted along the mid-plane of this laminate to create an initial delamination length of 63 mm. For all configurations, CNT sheets were only placed over half of the fabrics to fabricate CNT-reinforced and reference samples in one step; under identical processing conditions. After stacking, the preform dry fabrics were infused using resin transfer molding (RTM). The infusion was carried out at a volumetric flow rate of 5 cc/min while maintaining the infusion pressure at 2 bar. The mold and resin temperatures were held at 50 °C and 40 °C, respectively, during the RTM to ensure uniform infusion throughout the thickness. Composite specimens were cured at room temperature for 24 h, followed by a 2-h post-cure at 80 °C. Piano hinges were attached to the DCB samples using the epoxy-hardener mixture used as the matrix.

2.3. Testing

Fiber volume fraction was calculated following the ASTM D3171 Type II. This method assumes a zero void content, which is a reasonable assumption given that the void content in all examined samples was very low (see Supplementary materials Fig. S1 and S2 for cross-sectional images). The ASTM D792 was followed for density measurements.

An AmScope light microscope and an FEI Quanta 3D FEG scanning electron microscopy (SEM) were used to observe the specimens' fractured surfaces and internal structure. Cross-sectional samples (for failure type assessment) were cut in the middle perpendicular to the fiber direction and ground consecutively with 400, 600, 1000, and 1200 grit papers. This was followed by polishing using 1 μm diamond and 50 nm colloidal silica. Specimens were gold-coated for SEM to avoid charging.

X-ray micro-computed tomography (μCT) of fractured specimens was conducted on an Xradia microXCT at UTCT at the Univeristy of Texas at Austin. High resolution (8 μm/piexel) volumetric images covering a length and width of 10 mm and the entire thickness of the flexural samples were acquired for analysis. Dragonfly 4.0 was used to visualize the microstructure of each specimen [41].

The flexural properties of specimens were measured using the three-point bending test following the ASTM standard D790-17. For each configuration, seven specimens of 1.0 × 13.0 × 51.0 mm were tested on a span of 25.4 mm. The span to thickness ratio was chosen to prevent interlaminar shear failure in samples [42]. A constant crosshead displacement rate of 1.0 mm/min was applied, and each specimen was loaded until the crack propagated entirely through the specimen. Ten-millimeter diameter loading and support rollers were used to avoid crushing of the specimens under flexural loading.

SBS specimens were cut to 35.0 × 13.0 × 3.0 mm. SBS testing was performed following the ASTM D2344 with a slight increase in span to thickness ratio, taken as 6 instead of 4, to prevent local crushing and induce a large zone of uniform shear stress. Additionally, to avoid local stress concentration due to loading, a 10 mm loading cylinder and 3 mm support cylinders were used. For each configuration, seven samples were tested on a span of 18 mm under a constant crosshead displacement rate of 1 mm/min. Load and displacement were recorded until cracks propagated from the center to the edge of each sample.

Mode I interlaminar fracture toughness was evaluated using the double cantilever beam (DCB) test. Five specimens were tested for each configuration following the ASTM D 5528. The specimens were cut to 150.0 × 25.0 × 3.0 mm and loaded via clamped hinges in tension at a rate of 1 mm/min. A 24-megapixel camera (Canon EOS 80D) with a magnifying lens (Canon EF-S 18–200 mm lens) was used to record the crack propagation. Each specimen was initially loaded until the crack initiated and propagated 5 mm and was unloaded at a rate of 10 mm/min. The specimen was again loaded at a 1 mm/min rate until the final delamination reached 50 mm. Modified beam theory was applied to calculate the crack propagation's energy release rate for the crack's corrected length.

The electrical conductivity of the specimens in the fiber direction was measured using a DC two-probe method. A sample size of 50.0 ×

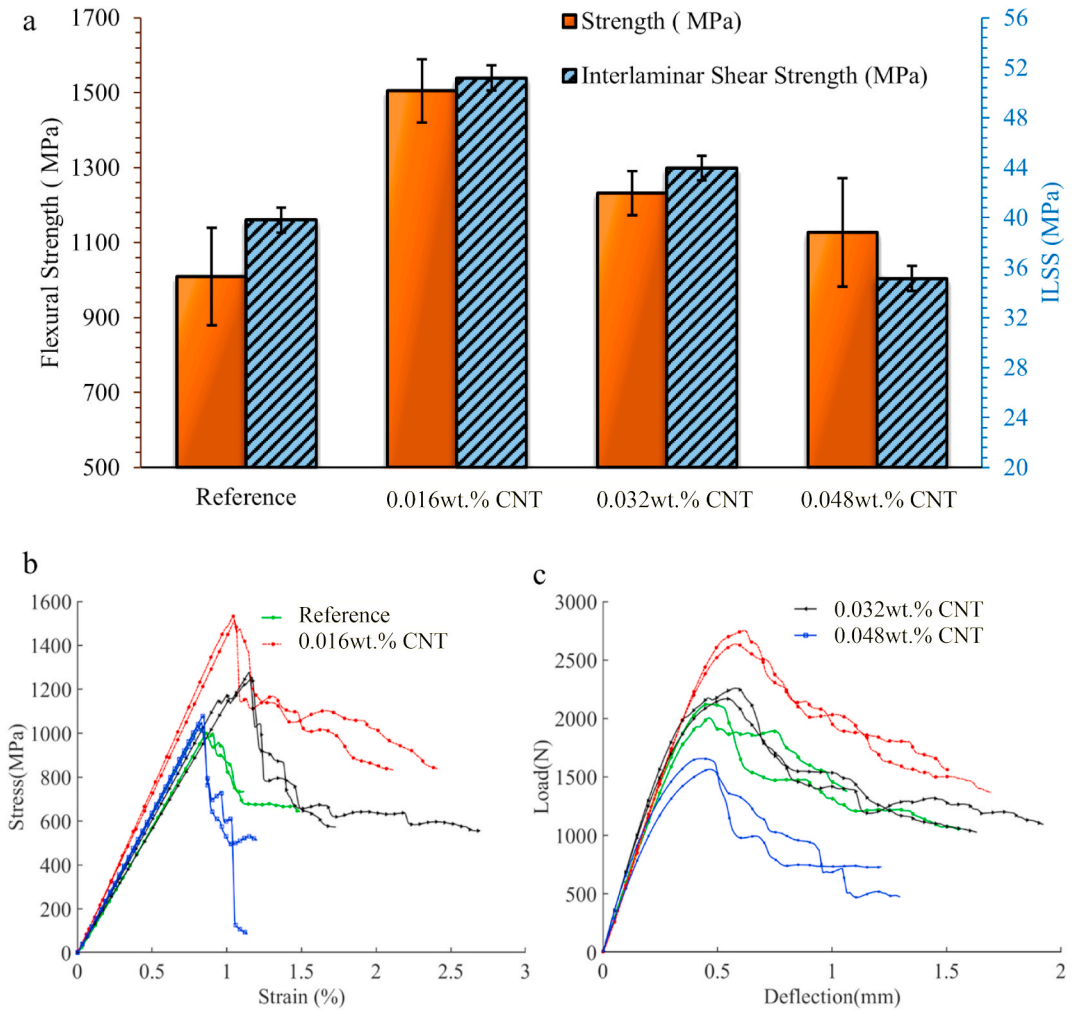

Fig. 2. a) Flexural and interlaminar properties of reference and CNT interleaved samples. b) Representative stress-strain plots of b) flexural stress-strain and c) load-displacement SBS testing.

13.0 × 1.0 mm was used. A Keithley 6221 DC and AC current source with a 2182A nano-voltmeter were used to measure electrical resistance. A conductive silver paste was applied at the point of contact between the specimen and electrical leads to reduce contact resistance. The voltage and current were recorded, and resistivity was calculated using the specimen dimensions.

3. Results and discussion

Cross-sectional graphs showed no structural difference between the reference and CNT-interleaved samples in the inter- or intra-laminar regions (Supplementary Material Figure S2). Moreover, there was no difference in the fiber volume fractions, ranging from 48 to 51%, between the reference and interleaved samples. It is reasonable to conclude that the interlaminar CNT sheets did not affect the RTM process. This was expected as the CNT sheets are <100 nm thick. The interlaminar CNTs in specimens were not detected under SEM due to their low contrast compared with the epoxy matrix.

Flexural strength and ILSS for the reference and interleaved samples are plotted in Fig. 2. The introduction of two interlaminar CNT sheets (0.016 wt%), at all interlaminar interfaces, increased the flexural strength by 49%, from 1009 to 1505 MPa. Specimens with four (0.032 wt%) and six (0.048 wt%) interlaminar CNT sheets, at all interlaminar interfaces, were stronger in flexure by 22% and 12% than the reference sample, respectively. The improvements were, however, lower than that realized by the addition of only two interlaminar CNT sheets. A similar trend for the ILSS was observed. Specimens with two interlaminar CNT sheets, at all interlaminar interfaces, achieved an ILSS that was 30% better than the reference. However, a higher number of interlaminar CNT sheets did not further improve the ILSS. Notably, six interlaminar sheets degraded the overall ILSS compared with the reference specimens. As expected, higher number of CNT sheets, stacked on top of each other, results in CNT agglomeration and prevents the resin to reach all CNTs during composite fabrication. ILSS trend in Fig. 2(a) suggests that CNT sheets enhance adhesion between fibers and matrix at the interlaminar interfaces; note that the two interlaminar CNT sheets are attached individually to the two laminates that form the sides of the interlaminar interface.

The representative stress-strain curves for the flexural tests and load-displacement curves for the SBS tests are depicted in Fig. 2(b) and (c). The flexural stress increases linearly up to the failure stress for all specimens. These plots indicate that the CNT-reinforced specimens fail at higher stresses/strains and can carry loads after the initial flexural failure. This observation is later explained in light of failure mechanisms. The initial stress drop after the peak stress is due to the fracture of the first laminate (top laminate), as confirmed by cross-sectional imaging of specimens (Supplementary Material Fig. S5). The SBS load-deflection curve in Fig. 2(b) indicates interlaminar shear failure followed by laminate crushing under the loading cylinder. The interfacial shear failure usually initiates in the midplane (where shear stress is maximum) or its adjacent interfaces and propagates through that same interface. For the specimens with 0.048 wt% CNTs (six interlaminar CNT

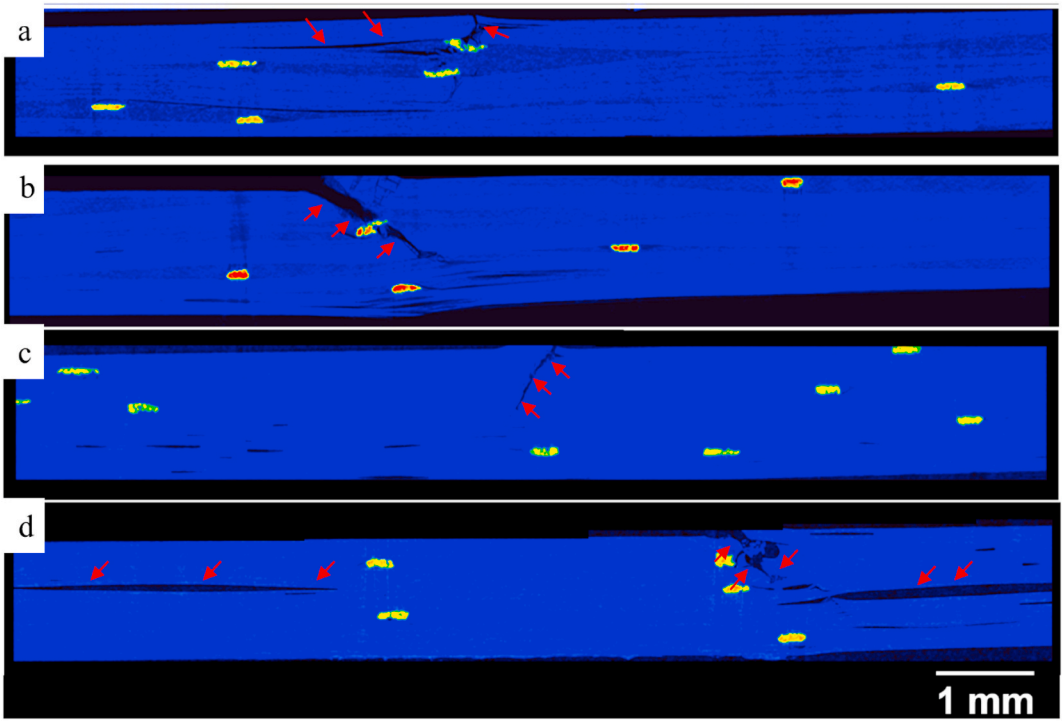

Fig. 3. μCT images of flexural specimens: a) Reference, reinforced with b) two (0.016 wt%), c) four (0.032 wt%), and d) six (0.048 wt%) CNT sheets, respectively.

sheets), failure occurs in several interfaces and propagates towards the edges at these interfaces (confirmed through μCT results as discussed later). Failure of multiple interlaminar interfaces suggests CNT agglomeration at the interlaminar interfaces. CNT agglomeration is not typical for low CNT loadings, however, in this study CNT sheets are concentrated at the CFRP's interlaminar regions, achieving high local loadings at those interfaces.

ILSS depends on the combined shear properties of the matrix and the interfacial bonding between fibers and the matrix. The changes in ILSS can, therefore, can be explained in terms of improvement or degradation of the matrix and the fiber-matrix interface properties due to interlaminar CNT sheets. As noted earlier, no apparent difference between the microstructures of the reference and CNT-reinforced specimens was found. The two CNT sheets (0.016 wt%, one adjacent to each carbon fiber fabric) improve both the shear properties of the matrix in their vicinity and the fiber-matrix adhesion by increasing the fiber surface area [43]. Most studies use CNTs that are only tens of microns and thus are minimally effective in strengthening their host matrix. The CNTs used in this study were 0.3 mm long (aspect ratio of 30,000) and, therefore, highly effective in locally improving the matrix's strength [44]. It has been shown that wrapping individual carbon fibers with CNT sheets (similar to the sheets used in this study) can significantly improve the matrix shear properties adjacent to the fibers, thus improving the fiber-matrix adhesion [43]. The stacked CNT sheets (in 4 and 6 interlaminar CNT sheets samples) are not thoroughly infused with the polymer due to agglomeration [45,46]. As a result, they can slide against each other, resulting in lower flexural and SBS properties compared with the samples with only two interlaminar CNT sheets. In summary,

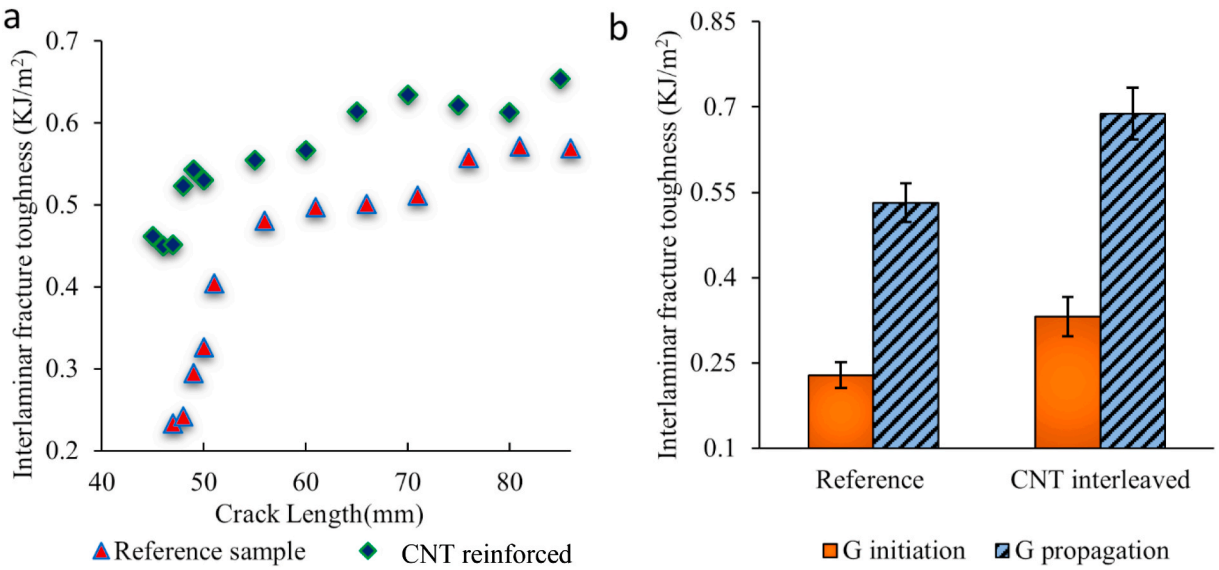

Fig. 4. a) R-curve . and b) Fracture toughness values during crack initiation and propagation for the reference sample and samples with two interlaminar CNT sheets.

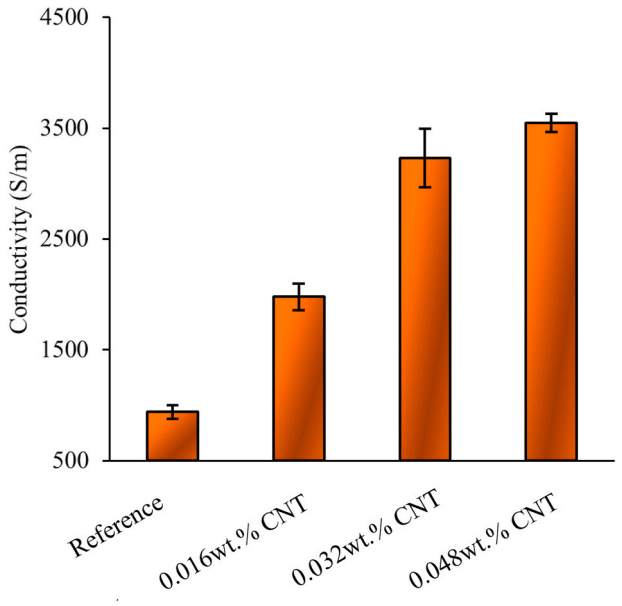

Fig. 5. The electrical conductivity of the reference and CNT-reinforced specimens.

interlaminar CNT sheets improve (i) the strength of the matrix at the interlaminar regions and (ii) enhance the fiber-matrix adhesion at the interlaminar interfaces. These two mechanisms result in an improved ILSS.

To study the effect of CNT alignment, specimens with interlaminar CNT sheets perpendicular to the fiber directions were also fabricated and tested (Supplementary Material Fig. S3). As expected, a similar degree of improvement was found when the aligned CNT sheets were perpendicular to the fibers in the unidirectional coupons. This confirms that CNTs do not affect the fiber-dominated properties but rather the matrix-dominated and fiber-matrix properties.

Failure mechanisms in flexural tests were studied using optical microscopy and μCT imaging, as shown in Supplementary Material Fig. S4, S5, and Fig. 3. Cracks in all specimens started on the compression side, as the compressive strength of CFRPs is typically lower than their tensile strength (Supplementary Material Fig. S5). Kink bands were observed in all tested specimens, an example of which is shown in Supplementary Material Fig. S4. Fig. 3 (a) displays cracks in the reference specimen that are initiated on the top surface (compressive side), propagating vertically through one laminate, and continue progressing in the interlaminar region, resulting in a mixed failure mode. For the specimens containing two (0.016 wt%) or four (0.032 wt%) interlaminar CNT sheets, cracks were found to continue to propagate through the entire thickness towards the last laminate as shown in Fig. 3 (b) and Fig. 3 (c). Partial interlaminar cracks are observed in these sample sets. For the specimens with six (0.048 wt%) interlaminar CNT sheets, the interlaminar cracks initiated in addition to compressive failure at the top. This failure mode is supported by the low ILSS of the samples with six interlaminar CNT samples at all their interlaminar interfaces. Based on the discussed failure mechanisms, the interleaved samples' enhanced flexural strength is due to both a higher ILSS and ability to resist crack initiation and growth.

Fracture toughness measurements were conducted to quantitatively assess the ability of CNT interleaved specimens to resist the initiation and progression of cracks in mode I. The maximum load carried by the reference specimen in the DCB test was 43±8 N, whereas the CNT interleaved specimens carried a maximum load of 57±3 N. Fig. 4 shows a typical resistance curve (R-curve) for the reference and two interlaminar CNT sheets samples. The far-left data points in Fig. 4 (a) show that the G_I is higher during crack initiation for the specimen interleaved with CNT sheets, indicating that interlaminar CNT sheets improve crack initiation resistance. The rising R-curve values signify unstable crack growth in both specimen types. Fig. 4(b) summarizes the initiation and propagation of interlaminar fracture toughness values for the reference and CNT-reinforced samples. The GI value for crack lengths in the 65–75 mm range is taken as the propagation fracture toughness. The mode I fracture toughness of interlaminar CNT sample for crack initiation and propagation was improved by 57% and 30%, respectively, over the reference sample.

The electrical conductivity of the reference and interleaved specimens measured in the carbon fiber direction is shown in Fig. 5. The electrical conductivity increases with the number of interlaminar CNT sheets. Although the volume fraction of CNT sheets is minuscule, their high conductivity compared with the carbon fibers results in an overall improvement of the electrical conductivity. The improved conductivity has implications for electromagnetic interference (EMI) shielding, lightning strike protection, and de-icing [47].

4. Conclusions

Interlaminar CNT sheets (with <0.05 wt% loadings) were investigated for increasing the flexural and interlaminar mechanical properties of CFRPs. The addition of CNT sheets improved the electrical conductivity of the tested samples. Significant improvements in flexural, ILSS, and fracture toughness of specimens were achieved for almost no penalty in weight, cost, thickness, or manufacturing. Two interlaminar CNT sheets placed at each interlaminar interface (0.016 wt% CNT loading) resulted in the most considerable improvements in CFRP's mechanical properties. Higher loadings were not effective in further enhancing the studied mechanical properties due to agglomeration, preventing proper infusion of the CNTs. The results show that the aligned CNT sheets prevent crack propagation along the interlaminar region. These sheets also improved interlaminar load transfer and fiber-matrix interaction in the interlaminar region. In conclusion, dry spun CNT sheets can be simply integrated with the composite manufacturing processes to improve CFRPs' interlaminar properties without changing their weight, thickness, or microstructure.

Author contribution

Pratik Koirala: Writing – review & editing, Writing – original draft, Formal analysis/testing, Methodology, Nekoda van de Werken: Writing – review & editing, Formal analysis/testing, Hongbing Lu: Writing – review & editing, Conceptualization, Funding acquisition, Ray H. Baughman: Writing – review & editing, Funding acquisition, Conceptualization, Raquel Ovalle-Robles: Writing – review & editing, Mehran Tehrani: Writing – review & editing, Supervision/administration, Funding acquisition, Writing – original draft, Methodology, Conceptualization.

Declaration of competing interest

The authors declare that they have no known competing financial interests or personal relationships that could have appeared to influence the work reported in this paper.

Acknowledgments

This work was supported under the NSF CAREER award CMMI-2015732. Tehrani gratefully acknowledges the support. Lu and Baughman at the University of Texas at Dallas acknowledge NSF's support under CMMI-1636306 and CMMI-1726435. Lu also acknowledges the additional support by the Beecherl endowed chair. The authors acknowledge Pouria Khanbolouki for his helo with the figures.

Appendix A. Supplementary data

Supplementary data to this article can be found online at https://doi.org/10.1016/j.compositesb.2021.108842.

References

[1] Cheng XY, Yokozeki T, Wu LX, Wang HP, Zhang JM, Koyanagi J, et al. Electrical conductivity and interlaminar shear strength enhancement of carbon fiber reinforced polymers through synergetic effect between graphene oxide and polyaniline. Compos Part a-Appl S 2016;90:243–9.

[2] Cheng XY, Zhang JM, Wang HP, Wu LX, Sun QF. Improving the interlaminar shear strength and thermal conductivity of carbon fiber/epoxy laminates by utilizing the graphene-coated carbon fiber. J Appl Polym Sci 2019;136(7).

[3] Fan Z, Santare MH, Advani SG. Interlaminar shear strength of glass fiber reinforced epoxy composites enhanced with multi-walled carbon nanotubes. Compos Appl Sci Manuf 2008;39(3):540–54.

[4] Khan SU, Kim JK. Improved interlaminar shear properties of multiscale carbon fiber composites with bucky paper interleaves made from carbon nanofibers. Carbon 2012;50(14):5265–77.

[5] Beckermann GW. Nanofiber interleaving veils for improving the performance of composite laminates. Reinforc Plast 2017;61(5):289–93.

[6] Beylergil B, Tanoğlu M, Aktaş E. Enhancement of interlaminar fracture toughness of carbon fiber–epoxy composites using polyamide-6, 6 electrospun nanofibers. J Appl Polym Sci 2017;134(35):45244.

[7] De Schoenmaker B, Van der Heijden S, De Baere I, Van Paepegem W, De Clerck K. Effect of electrospun polyamide 6 nanofibres on the mechanical properties of a glass fibre/epoxy composite. Polym Test 2013;32(8):1495–501.

[8] Hamer S, Leibovich H, Green A, Avrahami R, Zussman E, Siegmann A, et al. Mode I and Mode II fracture energy of MWCNT reinforced nanofibrilmats interleaved carbon/epoxy laminates (vol 90, pg 48, 2014). Compos Sci Technol 2014;93:114.

[9] Wang YL, Pillai SKR, Che JF, Chan-Park MB. High interlaminar shear strength enhancement of carbon fiber/epoxy composite through fiber- and matrix-anchored carbon nanotube networks. Acs Appl Mater Inter 2017;9(10):8960–6.

[10] Zhou HLZ, Du XS, Liu HY, Zhou HM, Zhang Y, Mai YW. Delamination toughening of carbon fiber/epoxy laminates by hierarchical carbon nanotube-short carbon fiber interleaves. Compos Sci Technol 2017;140:46–53.

[11] Gojny FH, Wichmann MH, Fiedler B, Bauhofer W, Schulte K. Influence of nano-modification on the mechanical and electrical properties of conventional fibre-reinforced composites. Compos Appl Sci Manuf 2005;36(11):1525–35.

[12] Han X, Zhao Y, Sun J-m, Li Y, Zhang J-d, Hao Y. Effect of graphene oxide addition on the interlaminar shear property of carbon fiber-reinforced epoxy composites. N Carbon Mater 2017;32(1):48–55.

[13] Tehrani M, Boroujeni A, Hartman T, Haugh T, Case S, Al-Haik M. Mechanical characterization and impact damage assessment of a woven carbon fiber reinforced carbon nanotube–epoxy composite. Compos Sci Technol 2013;75:42–8.

[14] Tehrani M, Safdari M, Boroujeni A, Razavi Z, Case S, Dahmen K, et al. Hybrid carbon fiber/carbon nanotube composites for structural damping applications. Nanotechnology 2013;24(15):155704.

[15] Wong DW, Lin L, McGrail PT, Peijs T, Hogg PJ. Improved fracture toughness of carbon fibre/epoxy composite laminates using dissolvable thermoplastic fibres. Compos Appl Sci Manuf 2010;41(6):759–67.

[16] Sohn M, Hu X, Kim J, Walker L. Impact damage characterisation of carbon fibre/epoxy composites with multi-layer reinforcement. Compos B Eng 2000;31(8):681–91.

[17] Yao HC, Zhou GD, Wang WT, Peng M. Effect of polymer-grafted carbon nanofibers and nanotubes on the interlaminar shear strength and flexural strength of carbon fiber/epoxy multiscale composites. Compos Struct 2018;195:288–96.

[18] Park JK, Lee JY, Drzal LT, Cho D. Flexural properties, interlaminar shear strength and morphology of phenolic matrix composites reinforced with xGnP-coated carbon fibers. Carbon Lett 2016;17(1):33–8.

[19] Du XS, Zhou HLZ, Sun WF, Liu HY, Zhou GN, Zhou HM, et al. Graphene/epoxy interleaves for delamination toughening and monitoring of crack damage in carbon fibre/epoxy composite laminates. Compos Sci Technol 2017;140:123–33.

[20] Zhao LJ, Zhang FP, Hu XZ, Huang BZ. Study on interlaminar shear and damage behavior of carbon fiber composites with short fiber interleaves: 1. The comparative test. Adv Mater Res-Switz. 2008;41–42. 335-+.

[21] Liu N, Wang JZ, Yang J, Han GF, Yan FY. Effects of nano-sized and micro-sized carbon fibers on the interlaminar shear strength and tribological properties of high strength glass fabric/phenolic laminate in water environment. Compos B Eng 2015;68:92–9.

[22] Fu S-Y, Lauke B. Characterization of tensile behaviour of hybrid short glass fibre/calcite particle/ABS composites. Compos Appl Sci Manuf 1998;29(5–6):575–83.

[23] Fu S-Y, Feng X-Q, Lauke B, Mai Y-W. Effects of particle size, particle/matrix interface adhesion and particle loading on mechanical properties of particulate–polymer composites. Compos B Eng 2008;39(6):933–61.

[24] Alessi S, Di Filippo M, Dispenza C, Focarete ML, Gualandi C, Palazzetti R, et al. Effects of Nylon 6, 6 nanofibrous mats on thermal properties and delamination behavior of high performance CFRP laminates. Polym Compos 2015;36(7):1303–13.

[25] Daelemans L, van der Heijden S, De Baere I, Rahier H, Van Paepegem W, De Clerck K. Nanofibre bridging as a toughening mechanism in carbon/epoxy composite laminates interleaved with electrospun polyamide nanofibrous veils. Compos Sci Technol 2015;117:244–56.

[26] Daelemans L, van der Heijden S, De Baere I, Rahier H, Van Paepegem W, De Clerck K. Using aligned nanofibres for identifying the toughening micromechanisms in nanofibre interleaved laminates. Compos Sci Technol 2016;124:17–26.

[27] Storck S, Malecki H, Shah T, Zupan M. Improvements in interlaminar strength: a carbon nanotube approach. Compos B Eng 2011;42(6):1508–16.

[28] Zhao Z, Teng K, Li N, Li X, Xu Z, Chen L, et al. Mechanical, thermal and interfacial performances of carbon fiber reinforced composites flavored by carbon nanotube in matrix/interface. Compos Struct 2017;159:761–72.

[29] Boroujeni AY, Tehrani M, Nelson AJ, Al-Haik M. Effect of carbon nanotubes growth topology on the mechanical behavior of hybrid carbon nanotube/carbon fiber polymer composites. Polym Compos 2016;37(9):2639–48.

[30] Tehrani M, Boroujeni AY, Luhrs C, Phillips J, Al-Haik MS. Hybrid composites based on carbon fiber/carbon nanofilament reinforcement. Materials 2014;7(6):4182–95.

[31] van der Heijden S, Daelemans L, De Schoenmaker B, De Baere I, Rahier H, Van Paepegem W, et al. Interlaminar toughening of resin transfer moulded glass fibre epoxy laminates by polycaprolactone electrospun nanofibres. Compos Sci Technol 2014;104:66–73.

[32] Wang G, Yu D, Kelkar AD, Zhang L. Electrospun nanofiber: emerging reinforcing filler in polymer matrix composite materials. Prog Polym Sci 2017;75:73–107.

[33] Aruchamy K, Mahto A, Nataraj S. Electrospun nanofibers, nanocomposites and characterization of art: insight on establishing fibers as product. Nano-Structures & Nano-Objects 2018;16:45–58.

[34] Garcia EJ, Wardle BL, Hart AJ. Joining prepreg composite interfaces with aligned carbon nanotubes. Compos Part a-Appl S 2008;39(6):1065–70.

[35] Palazzetti R, Zucchelli A, Trendafilova I. The self-reinforcing effect of Nylon 6, 6 nano-fibres on CFRP laminates subjected to low velocity impact. Compos Struct 2013;106:661–71.

[36] Daelemans L, van der Heijden S, De Baere I, Rahier H, Van Paepegem W, De Clerck K. Improved fatigue delamination behaviour of composite laminates with electrospun thermoplastic nanofibrous interleaves using the Central Cut-Ply method. Compos Part a-Appl S 2017;94:10–20.

[37] Arai M, Hirokawa J-i, Hanamura Y, Ito H, Hojo M, Quaresimin M. Characteristic of mode I fatigue crack propagation of CFRP laminates toughened with CNF interlayer. Compos B Eng 2014;65:26–33.

[38] Ou YF, Gonzalez C, Vilatela JJ. Interlaminar toughening in structural carbon fiber/epoxy composites interleaved with carbon nanotube veils. Compos Part a-Appl S 2019;124.

[39] Zhang M, Fang S, Zakhidov AA, Lee SB, Aliev AE, Williams CD, et al. Strong, transparent, multifunctional, carbon nanotube sheets. Science 2005;309(5738):1215–9.

[40] Kim SH, Haines CS, Li N, Kim KJ, Mun TJ, Choi C, et al. Harvesting electrical energy from carbon nanotube yarn twist. Science 2017;357(6353):773–8.

[41] Object research systems (ORS) Inc M, Canada. Dragonfly 4.0. 2018.

[42] Moreno MCS, Gutierrez AR, Vicente JLM. Flexural testing on carbon fibre laminates taking into account their different behaviour under tension and compression. Iop Conf Ser-Mat Sci 2016;139.

[43] Ravindranath PK, Roy S, Unnikrishnan V, Wang X, Xu T, Baughman R, et al. A multiscale model to study the enhancement in the compressive strength of multi-walled CNT sheet overwrapped carbon fiber composites. Compos Struct 2019;219:170–8.

[44] Van de Werken N, Reese MS, Taha MR, Tehrani M. Investigating the effects of fiber surface treatment and alignment on mechanical properties of recycled carbon fiber composites. Compos Appl Sci Manuf 2019;119:38–47.

[45] Filleter T, Yockel S, Naraghi M, Paci JT, Compton OC, Mayes ML, et al. Experimental-computational study of shear interactions within double-walled carbon nanotube bundles. Nano Lett 2012;12(2):732–42.

[46] Paci JT, Furmanchuk A, Espinosa HD, Schatz GC. Shear and friction between carbon nanotubes in bundles and yarns. Nano Lett 2014;14(11):6138–47.

[47] Katunin A, Krukiewicz K, Turczyn R, Sul P, Bilewicz M. Electrically conductive carbon fibre-reinforced composite for aircraft lightning strike protection. In: IOP conference series: materials science and engineering. IOP Publishing; 2017, 012008.